

# Asymmetrical flow field flow fractionation methods to characterize submicron particles: application to carbon-based aggregates and nanoplastics

Julien Gigault<sup>1</sup>  · Hind El Hadri<sup>2</sup> · Stéphanie Reynaud<sup>2</sup> · Elise Deniau<sup>2</sup> · Bruno Grassl<sup>2</sup>

Received: 29 July 2017 / Revised: 30 August 2017 / Accepted: 7 September 2017 / Published online: 25 September 2017  
© Springer-Verlag GmbH Germany 2017

**Abstract** In the last 10 years, asymmetrical flow field flow fractionation (AF4) has been one of the most promising approaches to characterize colloidal particles. Nevertheless, despite its potentialities, it is still considered a complex technique to set up, and the theory is difficult to apply for the characterization of complex samples containing submicron particles and nanoparticles. In the present work, we developed and propose a simple analytical strategy to rapidly determine the presence of several submicron populations in an unknown sample with one programmed AF4 method. To illustrate this method, we analyzed polystyrene particles and fullerene aggregates of size covering the whole colloidal size distribution. A global and fast AF4 method (method O) allowed us to screen the presence of particles with size ranging from 1 to 800 nm. By examination of the fractionating power  $F_d$ , as proposed in the literature, convenient fractionation resolution was obtained for size ranging from 10 to 400 nm. The global  $F_d$  values, as well as the steric inversion diameter, for the whole colloidal size distribution correspond to the predicted values obtained by model studies. On the basis of this method and without the channel components or mobile phase composition being changed, four isocratic subfraction

methods were performed to achieve further high-resolution separation as a function of different size classes: 10–100 nm, 100–200 nm, 200–450 nm, and 450–800 nm in diameter. Finally, all the methods developed were applied in characterization of nanoplastics, which has received great attention in recent years.

**Keywords** Field flow fractionation · Colloidal materials · Interlaboratory comparison · Nanoplastics

## Introduction

Characterization of colloidal particles, submicron particles, and other nanoparticles in aqueous systems is challenging even though it is essential for better control of the synthesis process, understanding their behavior in aqueous media, and evaluating their final transport mechanisms in environmental media [1–5]. The particle size distribution (PSD) of colloidal species (smaller than 1  $\mu\text{m}$ ) is a key parameter that can explain several mechanisms in aqueous media, such as aggregation [6, 7], dispersion [8, 9], and other transformations [10–12]. Therefore, its determination is a priority for researchers, and the precision of the measurement requires several validation tests [13].

To determine the size distribution of colloidal materials, dynamic light scattering (DLS) is one of the most popular routine techniques [13, 14]. Although the size distribution can be obtained rapidly and effectively by DLS, in the case of complex mixtures there may be several measurement biases due to the misinterpretation of the autocorrelation function and the size dispersity of the sample. The results obtained by DLS are generally user-dependent. Given that commercial instrument sellers and standardization process engineers turned this complex

**Electronic supplementary material** The online version of this article (<https://doi.org/10.1007/s00216-017-0629-7>) contains supplementary material, which is available to authorized users.

✉ Julien Gigault  
julien.gigault@univ-rennes1.fr

<sup>1</sup> Laboratoire Géosciences Rennes, UMR6118, CNRS – Université de Rennes 1, Av. Général Leclerc, Campus de Beaulieu, 35000 Rennes, France

<sup>2</sup> Institut des Sciences Analytiques et de Physico-chimie pour l'Environnement et les Matériaux, IPREM, UMR 5254, CNRS—Université de Pau et des Pays de l'Adour, 2 avenue P. Angot, Technopôle Hélioparc, 64000 Pau, France

technique into a “single-button” one, the sample size distribution is mostly obtained by means of a common procedure whatever the nature of the sample (without consideration of its specific features). Therefore, basic knowledge of light scattering (LS) is required for colloidal characterization, such as sample concentration and physical properties (refractive index of the sample and the solvent), baseline requirements (position and noise level), and stability of the sample. In the same way, proper algorithms have to be chosen for the autocorrelation function treatment, which strongly depends on the sample. Even if existing protocols are used to obtain the most accurate and efficient size determination, from consideration of all these requirements, the determination of the size distribution of a complex and/or unknown colloidal sample is highly challenging [15].

One interesting approach to determine an accurate and representative PSD consists in coupling a separation technique with use of several detectors, including LS detectors [16–19]. Of all the separation techniques, asymmetrical flow field flow fractionation (AF4) appears to have been the most promising approach in the last 10 years. On the basis of fluid dynamics and Fick’s law in a microscale channel, it is possible to separate analytes according to their diffusive properties (i.e., diffusion coefficient), which are directly proportional to their hydrodynamic size, ranging from a few nanometers to micrometers. Despite its broad separation range and its capacity to provide reliable size information in complex populations, AF4 is still considered a complex technique to set up so as to obtain rapid and robust size characterization of unknown submicron particle samples.

The objective of the present work was to demonstrate the feasibility of five different AF4 methods to rapidly (1) determine the presence of colloidal materials, (2) identify the different PSDs and dispersity, and (3) characterize the sample by LS according to the resolution of the fractionation method. To achieve our goals, different colloidal solutions, including fullerene aggregates and polystyrene latex (PSL) standard (particles with well-established PSD), were studied. Both samples were prepared to evaluate the fractionation efficiency according to the dispersity and the number of populations. The fractionation efficiency of the AF4 methods was previously assessed with use of the fractionating power ( $F_d$ ) by Williams [20, 21]. Finally, our method was applied to colloidal plastics, which are an emerging field for environmental and health safety programs. We hope that the proposed method will help researchers and engineers to rapidly and accurately characterize nanoscale and colloidal materials.

## Materials and methods

### Reagents

Sodium nitrate (catalog no. 229938) used to formulate the mobile phase was purchased from Sigma-Aldrich (Philadelphia,

PA, USA). Polyethersulfone (PES) filters (0.1  $\mu\text{m}$ , Pall®), purchased from VWR (Fontenay-sous-Bois, France) were used to remove particulates from the mobile phase. All solutions were prepared with ultrapure deionized water (18.2 M $\Omega$  cm, at 25 °C) obtained from a Milli-Q system (Millipore, France). Fullerene ( $C_{60}$ ) powder of more than 99.0% purity was purchased from VWR (Fontenay-sous-Bois, France). Triton X-100 was purchased from Sigma-Aldrich (Lyon, France). PSL beads (Thermo Scientific NIST traceable nanosphere size standards) were purchased from Fischer Scientific (Illkirch-Graffenstaden, France) with diameters of 80 nm (catalog no. 3080A), 125 nm (catalog no. 3125A), 400 nm (catalog no. 3400A), and 900 nm (catalog no. 3900A). Finally, a polystyrene-based nanoplastic solution (nano-PS; particles of plastics smaller than 1  $\mu\text{m}$ ) was produced by and purchased from Cordouan Technologies (Pessac, France; preparation protected by patent pending) and characterized by DLS and the zeta potential. PES ultrafiltration membranes of 10-kDa molecular mass cutoff were used for the 8200 Amicon stirred cell (Millipore, France), which was purchased from Alting (Metz, France). The other 0.2- and 0.45- $\mu\text{m}$  filters made with PES membranes used in the ultrafiltration cell were purchased from VWR (Fontenay-sous-Bois, France).

### Sample preparation

Fullerene nanoparticles were prepared as follows: 5 mg of  $C_{60}$  powder was placed in 20 mL of deionized water containing 0.02% w/w Triton X-100. The solution was left under vigorous magnetic stirring for 2 weeks. The solution changed from a suspension of black solids to a homogeneous brown-yellow solution, indicating the dispersion of fullerene aggregates ( $nC_{60}$ ). The solution was filtered through a PES filter with a 0.8- $\mu\text{m}$  membrane size cutoff, and the final solution obtained (named the “1–800 nm solution”) contained the whole  $nC_{60}$  colloidal population. Then, sequential ultrafiltration was performed with different membrane size cutoffs: 100-, 200-, and 450-nm PES membranes. The detailed protocol was presented in previous work [22]. Four fractions were obtained and named the “1–100-nm fraction,” “100–200-nm fraction,” “200–450-nm fraction,” and “450–800-nm fraction,” and correspond to the size limit of fullerene aggregates. In situ DLS (Vasco Flex, Cordouan Technologies, Pessac, France) was used to measure the size distribution of the particles in the bulk solution. Different mixed solutions were prepared by dilution of an optimal amount of each size of PSL beads with deionized water. The amount of each size of PSL beads was optimized to simulate a global size range representative of a finite number of monodisperse populations from 80 to 900 nm (DLS). Finally, the nano-PS sample was dispersed in an aqueous medium without any additives, and was first characterized by in situ DLS (Vasco Flex, Cordouan Technology, Pessac, France) (see Fig. S1).

## Instruments

The flow-mode analysis system used in this investigation consisted of an Eclipse 3+ AF4 instrument (Wyatt Technology, Dernbach, Germany) and a 1200 series high-performance liquid chromatography pump (Agilent Technologies, Les Ulis, France). A UV-vis absorption detector (1200 series, Agilent Technologies, Les Ulis, France) and a multiangle laser LS (MALS) detector (DAWN HELEOS, Wyatt Technology, Santa Barbara, CA, USA) formed the online detection system. Data from the detectors were collected and analyzed by ASTRA version 6 (Wyatt Technology, Santa Barbara, CA, USA). Data were saved in the native ASTRA format and then exported as text files for analysis, as described later.

## Methods

The AF4 channel thickness was fixed by a 250- $\mu\text{m}$  Mylar film, called a “spacer.” The channel dimensions were length 26.5 cm and width narrowing from 2.1 to 0.6 cm. The accumulation wall was defined by a 10-kDa PES membrane purchased from Wyatt Technology. To standardize the size fractionation approach, it is important to remove every step that requires modification and then clean the channel components. For instance, channel and mobile phase changes could definitely induce measurement bias and are time-consuming. In the case of positively charged colloidal particles, a cationic surfactant (such as cetyltrimethylammonium bromide) needs to be added to the mobile phase (the ionic strength remains constant) to prevent particles from sticking to the membrane. For all the AF4 conditions, the elution flow rate was fixed at 0.5 mL min<sup>-1</sup>, the injection flow rate was fixed at 0.2 mL min<sup>-1</sup>, and the sodium nitrate concentration of the mobile phase was fixed at 0.5 mmol L<sup>-1</sup>. The injection volume was chosen according to the concentration-based detector (UV detector). The focus-flow and cross-flow rates, during the relaxation and the elution, were optimized as a function of the size distribution of the sample, and are summarized in Table 1.

Online MALS measurements were conducted in a proper cell maintained at 20  $\pm$  0.1 °C. Because of the size limitation of the MALS system, and the fractal distribution for the whole colloidal size distribution, three formalisms of the light scattered were used: the Zimm formalism for particles with a radius of gyration ( $R_g$ ) less than 300 nm and angle ranging from 44° to 72°, the spherical formalism for particles with a geometric radius greater than 300 nm within the whole range of angles (50° to 134°), and the Berry formalism for nanoscale plastic  $R_g$  determination. The Berry method is the most appropriate formalism in terms of robustness and accuracy for hyperbranched materials [23]. Details concerning the relevancy of such formalisms have already been well documented [23]. Discrete measurement results are reported as the mean with an associated uncertainty of one standard deviation (presented as an interval or error bar), and are typically based on three to five replicates performed under repeatable conditions.

The selectivity  $S_d$  for field flow fractionation techniques measures the ability of a chromatographic technique to separate two components as expressed as

$$S_d = \frac{d \ln t_R}{d \ln d}, \quad (1)$$

where  $t_R$  is the retention time of the peak, and  $d$  is the nanoparticle diameter.

The analytical challenge for quantitative characterization of the whole colloidal size distribution is to obtain suitable selectivity (1) without loss of material on the membrane surface and (2) without the elution mode being changed from normal to steric. For programmed elution in AF4, the classical theoretical equation used to evaluate the fractionation such as by the linearity (time versus size illustrated by the selectivity) can no longer give an indication of the resolution. As recently proposed by Williams [20, 21] and for the cross-flow rate with an exponential decay in particular, the fractionating power ( $F_d$ ) is an important and robust parameter, and is expressed as

$$F_d = \frac{t_R}{4\sigma_t} \frac{d \ln t_R}{d \ln d} = \frac{t_R}{4\sigma_t} S_d,$$

**Table 1** Asymmetrical flow field flow fractionation (AF4) focus-flow and cross-flow conditions for the different AF4 methods (as a function of the corresponding size distribution) during the relaxation and elution steps

AF4 methods		Relaxation		Elution	
Fractionation method	Analyte size targeted (nm)	Focus-flow rate $V_f$ (mL min <sup>-1</sup> )	Duration (min)	Cross-flow rate $V_c$ (mL min <sup>-1</sup> )	Duration (min)
O	1–800	0.5	5	$V_c = 2e^{-0.27t}$	25
A	1–100	2.0	5	0.3	40
B	100–200	1.0	5	0.3	40
C	200–450	1.0	5	0.1	15
D	450–800	0.5	5	0.1	15

For all conditions, the detector flow rate was fixed at 0.5 mL min<sup>-1</sup> and the injection flow rate was fixed at 0.2 mL min<sup>-1</sup>.

where  $t_R$  is the retention time corresponding to the maximum peak,  $\sigma_t$  is the standard deviation of the peak measured at the half width based on the Gaussian profile of the peak, and  $d$  is the nanoparticle diameter. Compared with the selectivity used for the isocratic cross-flow rate,  $F_d$  measures the resolution that can be obtained across the breadth of the peak. As firstly introduced by Giddings et al. [24] for particle size separation, the fractionating power is defined as the resolution for two closely eluted monodisperse components divided by their relative difference in diameter.

## Results and discussion

### Programmed AF4 method applied to polydisperse $nC_{60}$

DLS is often used to rapidly screen the presence and the global size distribution of colloids in aqueous media. As a DLS method in the case of an unknown colloidal sample with no indication of the global size distribution, method O was first used to discriminate the presence of several populations. Fullerene nanoparticle aggregates were used as a test sample because of their polydispersity (continuum of sizes) and stability in aqueous media as previously demonstrated [24, 25]. Figure 1 presents the fractograms of the  $nC_{60}$  colloidal population with size covering the nanoscale (less than 1  $\mu\text{m}$ ) and the selectivity obtained according to the size range of the different purified subclasses (see “Materials and methods”).

It clearly appears that the whole colloidal size distribution can be fractionated within the first 20 min of analysis (Fig. 1a). As indicated in Table 1, the relaxation step is defined by a relatively low cross-flow rate (as compared with the initial cross-flow rate during the early stage of the elution step) of  $0.5 \text{ mL min}^{-1}$ . On the basis of the previously published protocol, this  $0.5 \text{ mL min}^{-1}$  cross-flow rate is sufficient to obtain a rapid overview of the whole colloidal size range without loss of materials on the membrane surface (i.e., recovery less than 80% based on the concentration detector) considering the presence of larger particles in the sample [22]. A too high focus-flow rate during the relaxation is, in our case, visualized by a typical mark on the membrane surface at the relaxation zone. After the relaxation time, a cross-flow rate with an exponential decay was optimized.

The rapid decrease of the cross-flow rate from  $2.0 \text{ mL}$  to  $0.1 \text{ mL min}^{-1}$  in the first 13 min allows fractionation of the size range from 1 to 200 nm in diameter with a selectivity starting at 0.99 and reaching 0.17. After these first 13 min, the rapid elution of the next population is due to the low cross-flow rate (from 0.1 to  $0 \text{ mL min}^{-1}$ ) exhibiting poor selectivity (less than 0.07). The selectivity decreases smoothly when the size is greater than 200 nm. As a result, two different regimes of separation can be identified when method O is applied. First, a high-resolution regime is observed for size (radius) ranging from 1 to 200 nm, and second, poor resolution is obtained for a radius greater than 200 nm. The

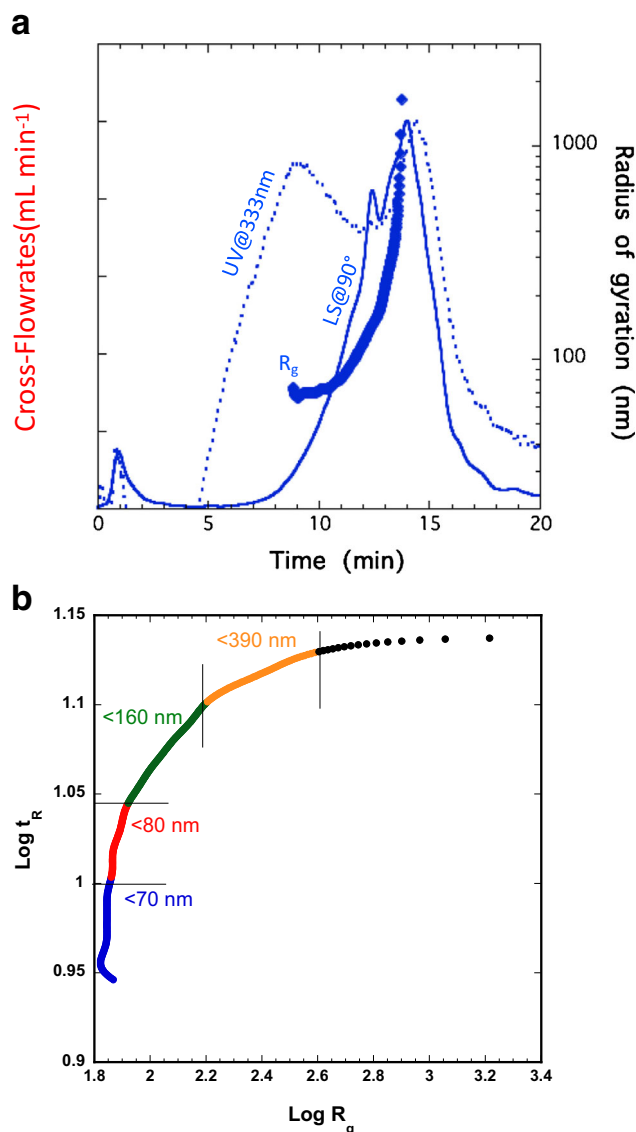


**Fig. 1** **a** Typical fractograms [light scattering (LS) detection at  $90^\circ$  and UV-vis detection at 333 nm] obtained for 1–800 nm with method O with variation of  $R_g$  as a function of the retention time ( $t_R$ ). **b** The corresponding selectivity for the different size regimes identified in **a** and defined as the slope of the linear variation between  $\log t_R$  as a function of  $\log R_g$ .

choice of the exponential decay is a powerful feature to highlight the presence of large particles without considering the size determination and sacrificing the fractionation resolution. As illustrated in Fig. 1, the presence of the size continuum cannot be totally characterized by LS detection. Although the cross-flow rate becomes close to zero after 13 min of analysis, all remaining particles are packet eluted. Such a phenomenon could create a co-elution phenomenon, and is responsible for the misunderstanding of the size determination and misinterpretation of the results. Nevertheless, method O still gives important information in a first approach with an overview of the overall elution profile even if the size variation should not be taken into account.

In addition to  $S_d$ ,  $F_d$  was determined for the different  $nC_{60}$  size-purified dispersions (with use of sequential ultrafiltration) after fractionation with method O (see the electronic supplementary material, Fig. S2).  $F_d$  was evaluated as  $1.0 \pm 0.1$ ,  $0.49 \pm 0.06$ ,  $0.29 \pm 0.03$ ,  $0.098 \pm 0.009$ , and  $0.37 \pm 0.05$  for the 1–100-nm, 100–200-nm, 200–450-nm, 450–800-nm, and 1–800-nm fractions, respectively. As expected,  $F_d$  tends to zero at the point of steric inversion [21, 26]. It appears that  $F_d$  obtained for the 1–800-nm fraction is a compromise between the values obtained for the 100–200-nm and 200–450-nm fractions. Compared with LS detectors, which are influenced by larger particles ( $r^6$ ), such  $F_d$  results indicated that this parameter is a more appropriate indicator to evaluate the fractionation efficiency of the AF4 method. As a result, method O appears to be optimal for fractionating and characterizing a large size distribution (1–800 nm). For similar fractionation conditions, it was predicted and modeled by Williams that  $F_d$  is 0.545 for 1 nm, 1.98 for 10 nm, and 0.496 for 100 nm [21]. Williams evaluated a steric inversion diameter greater than 1  $\mu\text{m}$ , which corresponds to the size variation and fractionation that we obtained by method O. The fractionating power for constant cross flow is relatively higher than that obtained for programmed cross flow.

Programmed AF4 method applied to a mixture of monodisperse PSL beads

We also analyzed three PSL samples with method O. The first sample contained only particles of 400-nm diameter, the second contained particles of 125- and 400-nm diameter, and the third contained particles of 80-, 125-, 400- and 900-nm diameter and was named the “80–900-nm sample.” The corresponding fractograms are reported in Fig. 2, with the variation of the geometric radius (determined by the spherical formalism since PSL beads are spheres). The 80–900-nm fractogram was realized in dilute conditions to avoid any co-elution phenomenon caused by interparticle interactions [27, 28]. Two regimes may be distinguished, one for size smaller than 200 nm and another for size greater than 200 nm, which confirms our previous observation for  $nC_{60}$  samples. Below 200 nm,  $F_d = 2.4 \pm 0.3$ , which is greater than the values obtained for the  $nC_{60}$  samples. This difference is because the PSL sample is a mixture of separate monodisperse particles, whereas the  $nC_{60}$  sample was made of a continuum of sizes. For the regime beyond 200 nm, as expected method O allows a rapid overview of the sample content, and the two populations (i.e., 125 and 400 nm; Fig. 2, plot b) are discriminated on the basis of the elution profile. However, method O cannot differentiate the larger size (900 nm) because of its low concentration and the limitation of LS to detect such diameters (Fig. 2, plot c). Between 200 and 400 nm,  $F_d$  is of the same order of magnitude,  $0.33 \pm 0.02$ . Method O appears to be highly valuable to identify the presence of aggregates of small particles, especially for nanoparticles (with dimension ranging from 1 to 100 nm).

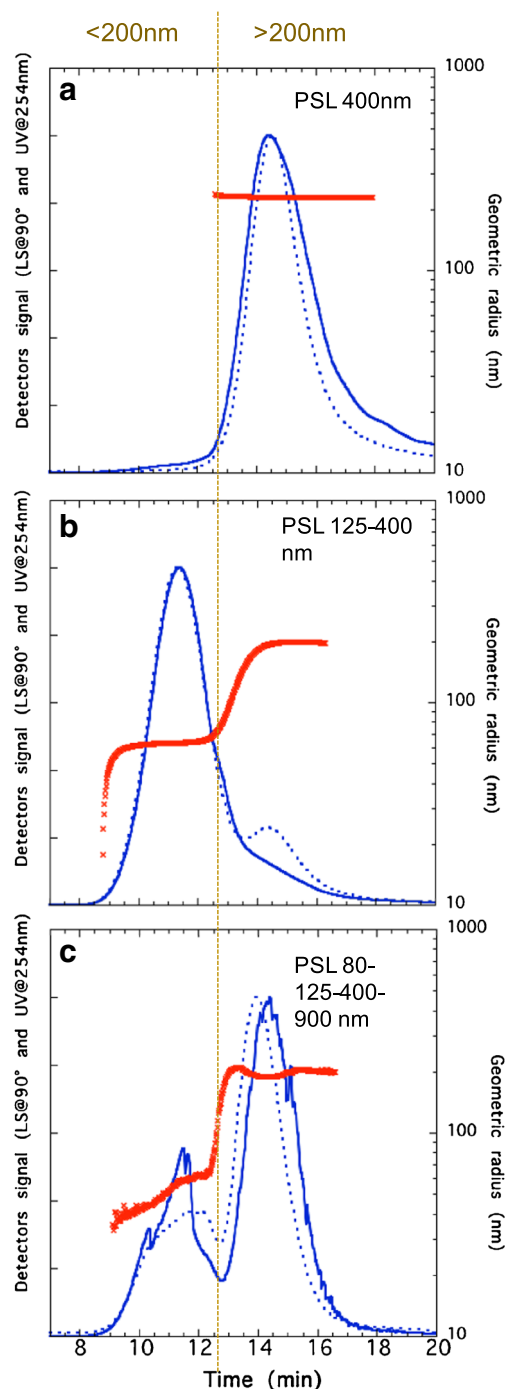


**Fig. 2** Typical fractograms [light scattering (LS) detection at  $90^\circ$  and UV–vis detection at 254 nm] obtained for three polystyrene latex (PSL) mixture solutions—PSL 400 nm (a), PSL 125 and 400 nm (b), PSL 80, 125, 400, and 900 nm (c) obtained with method O. The geometric radius variation as a function of the retention time, obtained from the spherical formalism, is plotted in red

### Isocratic AF4 methods applied to $nC_{60}$

The aim of our analytical strategy is to propose a fractionation method with no need for any change of the channel components and with a reasonable analysis duration. By keeping in

mind the results of method O, we went further and optimized four isocratic methods based on four size ranges and called “method A” for 1–100 nm, “method B” for 100–200 nm, “method C” for 200–450 nm, and “method D” for 450–800 nm. Because the cross-flow rate is kept constant during the whole elution step, the four AF4 methods were evaluated in terms of selectivity. In a first approach, an  $nC_{60}$  sample containing different particle sizes within the range 1–800 nm was prepared before being analyzed by AF4–UV–vis detection–MALS by the different methods.

To optimize methods A–D, two strategies were adopted according to the size range: 1–200-nm and greater than 200 nm. We mainly focused the method optimization on the relaxation process. From Fick’s law, the diffusion phenomenon occurring during the relaxation step is one of the most important processes to obtain an efficient fractionation. The focus-flow rate was decreased from 2.0 mL min<sup>-1</sup> for method A to 1.0 mL min<sup>-1</sup> for method B, and from 1.0 mL min<sup>-1</sup> for method C to 0.5 mL min<sup>-1</sup> for method D (Table 1). With a 250- $\mu$ m spacer thickness, an excessive cross-flow rate (above 1.5 mL min<sup>-1</sup>) during the relaxation and the elution could create a co-elution phenomenon by increasing the particle–membrane interaction and/or irreversible adsorption (loss of materials) onto the membrane surface. To validate the fractionation efficiency, the selectivity was determined. Figure 3 presents the fractograms (LS trace) of the 1–800-nm solution obtained with method O (green trace) and the four specific methods: A, B, C, and D (blue lines); the selectivity is also reported.  $S_d$  in blue corresponds to the specific method (methods A–D), whereas  $S_d$  in green corresponds to the equivalent  $S_d$  calculated from method O for the same size variation considered in the specific method.  $S_d$  appears to be more efficient for methods A–D than for the overall method (method O). This result could be related to the use of a constant cross-flow rate during the whole elution process for methods A–D.

Methods A and B are more appropriate for diameters below 200 nm to fractionate the particles efficiently. With the fractionation conditions and the cross-flow rates, larger particles may not be eluted during the time of the analysis, and may remain in the channel. Such a phenomenon is visualized by a large peak when the cross flow is stopped at the end of elution (data not shown). This final step allows elution of all retained species that are not irreversibly stuck on the membrane surface. As illustrated in Fig. 3a, in the very low size regime (i.e.,  $R_g < 100$  nm), the selectivity is close to unity for both method A and method O. Nevertheless, compared with method A, the selectivity rapidly decreases, reaching 0.7 at 100-nm diameter and 0.2 at 200-nm diameter (Fig. 3b). For  $R_g$  greater than 200 nm, methods C and D allow fractionation of the large species with a considerable increase in the selectivity compared with method O. Nevertheless, such improved resolution in the large size regime required the use of a low cross-flow rate during the relaxation and elution steps. These cross-flow conditions are

not sufficient to let the particles diffuse and be discriminating in the channel height with size smaller than 100 nm and 200 nm for methods C and D, respectively. In these fractionation conditions, the small  $nC_{60}$  particles are considered as unretained species, and are eluted with the dissolved phase in the void time (clearly identified with the concentration detector).

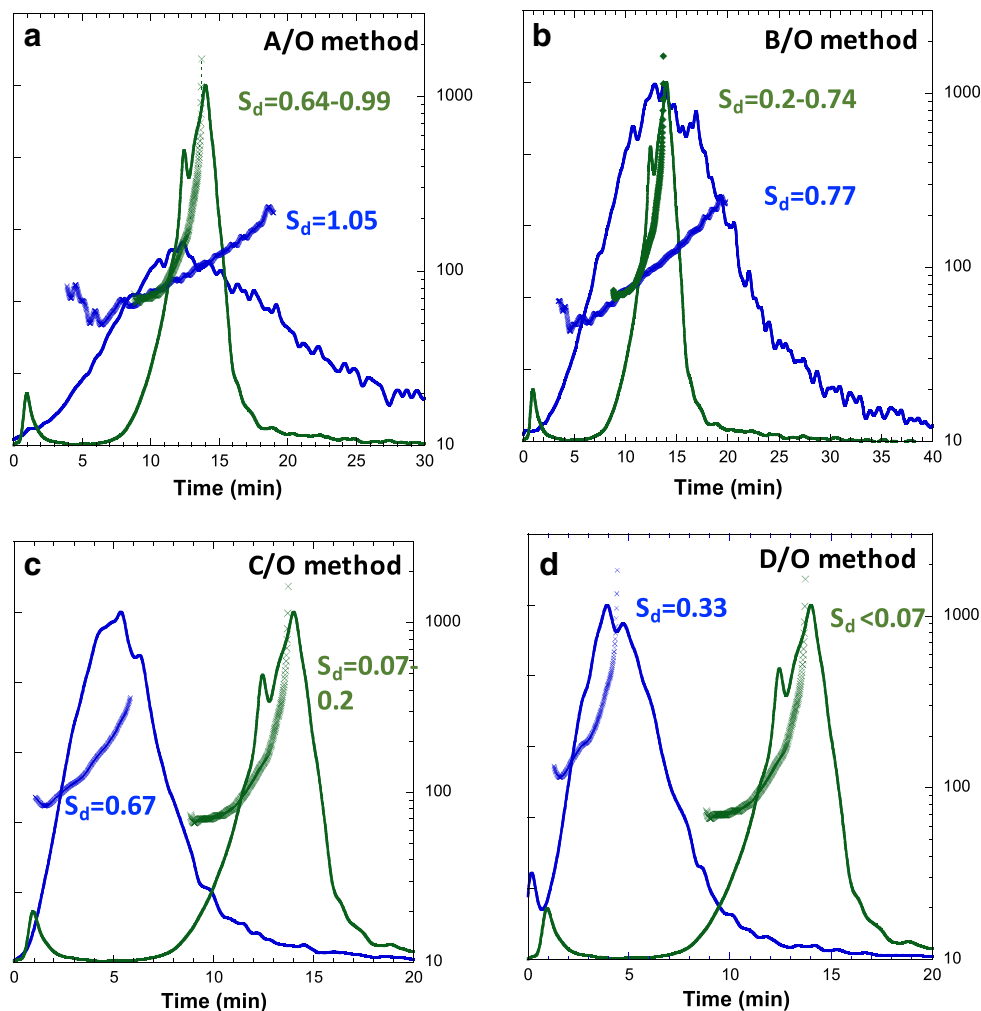
From these results, we propose a standard procedure to rapidly determine the presence of different colloidal populations in the solution in three steps as described below:

1. In a first step, it is recommended, if possible, to preanalyze the colloidal dispersion to determine the charge (zeta potential), the PSD (DLS in the bulk), and physicochemical properties of the medium such as pH and conductivity. This first analysis step allows determination of the global size distribution and the surface charge of the particles so as to optimize the mobile phase composition and anticipate the membrane–particle interactions. In our case, the  $nC_{60}$  sample has a negative zeta potential (data not shown) with a pH close to 6.0. In the case of positively charged colloids, it is necessary to add a cationic repulsive agent to the mobile phase to remove any electrostatic interaction on the membrane surface (which is globally negatively charged). The size distribution obtained by DLS on the bulk solution will provide crucial information about the possible presence of large aggregates interfering with the fractionation. In that case, prefiltration at 1  $\mu$ m ( $\pm 0.2$   $\mu$ m) just before AF4 analysis is required.
2. In a second step, method O is used to characterize the presence of submicron populations. As demonstrated, this method gives important information about the possible presence of colloidal populations, especially with size smaller than 200 nm. Then, the elution profile is typically different when particles with size ranging from 1 to 200 nm are present. Because of the high fractionating power at this size scale, the presence of small particles may be identified by AF4 but not by DLS (batch mode analysis) because of the contribution of the large particles to the scattered light.
3. In a third step, when the global population is identified, the subfraction methods (A–D) can be used to increase the size resolution and the population identification within the global colloidal population.

### Application of the method to nanoplastics

The method developed in the present study falls within the field of investigation of the environmental fate and behavior of anthropogenic nanoparticles [29]. Recently, research trying to solve the issues concerning the tracking of nanoparticles in environmental media has focused only on pristine materials without considering the transformation processes. As soon as

**Fig. 3** Fractograms (light scattering trace) of the 1–800-nm  $nC_{60}$  with the  $R_g$  variation as a function of the retention time realized with method O (green line) and compared with **a** method A, **b** method B, **c** method C, and **d** method D (blue line).  $S_d$  in blue corresponds to the specific method (methods A–D), whereas  $S_d$  in green corresponds to the equivalent  $S_d$  calculated from method O for the same size variation considered in the specific method



nanoparticles are produced, consumed, and released into the environment, they are subject to transformation processes changing the size, shape, and structure distribution. Generally, one of the most assumed processes is nanoparticle heteroaggregation according to the ionic strength, organic matter, and other natural colloidal materials [6]. Therefore, characterization of the whole colloidal size range appears to be one of the most challenging analytical developments for study of the environmental implications of anthropogenic nanomaterials. Of all the anthropogenic nanoparticles, we recently showed that nanoscale plastics are one of the hottest topics because of their possible release caused by degradation of microplastics [30–32]. Plastic litter has attracted the attention of scientific communities, public agencies, and the global population because of the gigantic amount of plastics produced and entering our environment every year. Recently, we demonstrated the occurrence of nanoscale plastics resulting from the degradation of millimeter-scale plastics by UV in the ocean, raising several urgent questions on their environmental and health impacts [33]. Figure 4 presents the AF4 results obtained for nanoscale plastics made to be used

for analytical development and ecotoxicology studies. Compared with PSL generally used for the same purposes, the large size distribution, the shape, and the fractal structure of the nanoscale plastics are similar to the those we observed and characterized from the UV degradation of microplastics sampled in the North Atlantic Gyre [33]. Characterizing accurately the size distribution of nanoscale plastics is therefore highly relevant. Our previous DLS results (see Fig. S1) present a continuum of sizes covering the whole nanoscale. Nevertheless, two populations were identified, with a large one from 200 to 600 nm in diameter and a relatively small fraction with hydrodynamic size centered around 70 nm (sparse Bayesian learning (SBL) algorithm). By application of method O (Fig. 4, plot a), a continuum of sizes is clearly identified for  $R_g$  from 80 nm up to several hundred nanometers. As for fullerene nanoparticles and PSL standards, with use of this method, the two-size regime can be identified in the fractograms, separated at  $R_g$  of 200 nm. The MALS and UV signals for  $R_g$  greater than 200 nm indicate a higher relative concentration than for the nanoscale plastics below this size limit. This result confirms our previous DLS characterization

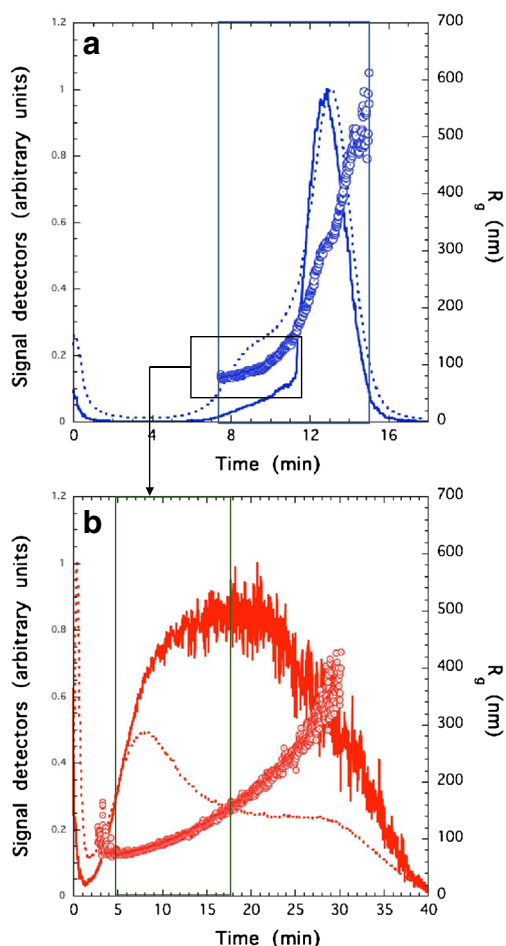


**Fig. 4** Fractograms of the nanoplastics prepared by Cordouan Technologies obtained with method O (a) and method A (b)

(see Fig. S1). Nanoscale plastics seem to be highly polydisperse with a continuum of sizes covering the whole colloidal size range. Because the resolution of the size separation and characterization is limited in the low size regime with method O and because the second population with  $R_g$  greater than 200 nm is more predominant, method A was further used to investigate the low size regime. Figure 4, plot b presents the fractograms of the solution of nanoplastics obtained in the conditions of method A. A large LS signal is identified, and corresponds to a broad and polydisperse population. Two UV peaks are identified, at 8.1 and 29.2 min. As observed by method O, the first population has  $R_g$  less than 200 nm. By use of method A, an increase in the size resolution characterization for the corresponding population is clearly demonstrated. For particles larger than 200 nm, a relative quantity is co-eluted and centered at 29.2 min.

The application of the methods to nanoscale plastics illustrates the potentiality of such an analytical approach for standardized measurements for interlaboratory comparison. With the considerable increase of interest of the scientific community in plastic litter, it is not necessary to repeat the errors made for engineered nanoparticles in terms of characterization

validation. Finally, methods A–D could be potentially relevant for coupling AF4 with inductively coupled plasma mass spectrometry to analyze a specific trace element associated with a specific size range.

## Conclusion

In this study, as predicted by recent theoretical study in the literature, we experimentally demonstrated different fractionation methods to characterize the whole colloidal size distribution of a polydisperse sample. The first objective was to obtain a rapid fractionation of the different submicron populations without our changing channel components and mobile phase composition and achieve high selectivity and fractionating power. With a single method, method O, we showed that it is possible to discriminate the presence of large particles (200–800 nm) from small particles (smaller than 200 nm) in a normal elution mode. Even if method O gives suitable selectivity in the low size regime, this decreases rapidly for diameters greater than 200 nm. Different subfractionation methods (methods A–D) with constant cross-flow rates were developed to increase the selectivity according to the small size range within the colloidal range. All these methods also validated the hypothesis made in the literature for different nanoscale (colloidal) materials. We hope that our work will stimulate researchers to use AF4 for characterization of highly environmentally challenging materials such as nanoscale plastics and other emerging nanoscale species.

**Compliance with ethical standards** The identification of any commercial product or trade names does not imply endorsement or recommendation by the French National Center for Scientific Research (CNRS).

**Conflict of interest** The authors declare that they have no competing interests.

## References

- Hassellöv M, Kaegi R. Analysis and characterization of manufactured nanoparticles in aquatic environments. In: Lead JL, Smith E, editors. Environmental and human health impacts of nanotechnology. Chichester: Wiley; 2009. p. 211–66.
- Tuoriniemi J, Johnsson ACJH, Holmberg JP, Gustafsson S, Gallego-Urrea JA, Olsson E, et al. Intermethod comparison of the particle size distributions of colloidal silica nanoparticles. *Sci Technol Adv Mater*. 2014;15:035009.
- Fedotov PS, Vanifatova NG, Shkinev VM, Spivakov BY. Fractionation and characterization of nano- and microparticles in liquid media. *Anal Bioanal Chem*. 2011;400:1787–804.
- Hassellöv M, Readman JW, Ranville JF, Tiede K. Nanoparticle analysis and characterization methodologies in environmental risk assessment of engineered nanoparticles. *Ecotoxicology*. 2008;17:344–61.



5. Tiede K, Boxall ABA, Tear SP, Lewis J, David H, Hasselov M. Detection and characterization of engineered nanoparticles in food and the environment. *Food Addit Contam Part A Chem Anal Control Expo Risk Assess.* 2008;25:795–821.
6. Hotze EM, Phenrat T, Lowry GV. Nanoparticle aggregation: challenges to understanding transport and reactivity in the environment. *J Environ Qual.* 2010;39:1909–24.
7. Petosa AR, Jaisi DP, Quevedo IR, Elimelech M, Tufenkji N. Aggregation and deposition of engineered nanomaterials in aquatic environments: role of physicochemical interactions. *Environ Sci Technol.* 2010;44:6532–49.
8. Andreev SM, Purgina DD, Bashkatova EN, Garshev AV, Maerle AV, Khaitov MR. Facile preparation of aqueous fullerene C60 nanodispersions. *Nanotechnol Russ.* 2014;9:369–79.
9. Jiang J, Oberdörster G, Biswas P. Characterization of size, surface charge, and agglomeration state of nanoparticle dispersions for toxicological studies. *J Nanopart Res.* 2009;11:77–89.
10. Dai M, Martin J-M, Cauwet G. The significant role of colloids in the transport and transformation of organic carbon and associated trace metals (Cd, Cu and Ni) in the Rhône delta (France). *Mar Chem.* 1995;51:159–75.
11. Pettibone JM, Gigault J, Hackley VA. Discriminating the states of matter in metallic nanoparticle transformations: what are we missing? *ACS Nano.* 2014;7:2491–9.
12. Hou WC, Jafvert CT. Photochemical transformation of aqueous C clusters in sunlight. *Environ Sci Technol.* 2009;43:362–7.
13. Baalousha M, Lead JR. Rationalizing nanomaterial sizes measured by atomic force microscopy, flow field-flow fractionation, and dynamic light scattering: sample preparation, polydispersity, and particle structure. *Environ Sci Technol.* 2012;46:6134–42.
14. Ross HF. Particle size analysis by dynamic light scattering. *Food Res Int.* 1994;27:159–8.
15. Hackley VA, Clogston JD. Measuring the size of nanoparticles in aqueous media using batch-mode dynamic light scattering. NIST special publication 1200-6. National Institute of Standards and Technology: Gaithersburg; 2007.
16. Baalousha M, Stolpe B, Lead JR. Flow field-flow fractionation for the analysis and characterization of natural colloids and manufactured nanoparticles in environmental systems: a critical review. *J Chromatogr A.* 2011;1218:4078–103.
17. Baalousha M, Lead JR. Size fractionation and characterization of natural aquatic colloids and nanoparticles. *Sci Total Environ.* 2007;386:93–102.
18. Lead JR, Wilkinson KJ. Aquatic colloids and nanoparticles: current knowledge and future trends. *Environ Chem.* 2006;3:159–71.
19. Lespes G, Gigault J. Hyphenated analytical techniques for multidimensional characterisation of submicron particles: a review. *Anal Chim Acta.* 2011;692:26–41.
20. Williams PS. Fractionating power and outlet stream polydispersity in asymmetrical flow field-flow fractionation. Part I: isocratic operation. *Anal Bioanal Chem.* 2016;408:3247–63.
21. Williams PS. Fractionating power and outlet stream polydispersity in asymmetrical flow field-flow fractionation. Part II: programmed operation. *Anal Bioanal Chem.* 2017;409:317–34.
22. Gigault J, Pettibone JM, Schmitt C, Hackley VA. Rational strategy for characterization of nanoscale particles by asymmetric-flow field flow fractionation: a tutorial. *Anal Chim Acta.* 2014;809:9–24.
23. Andersson M, Wittgren B, Wahlund K-G. Accuracy in multiangle light scattering measurements for molar mass and radius estimations. Model calculations and experiments. *Anal Chem.* 2003;75:4279–91.
24. Giddings JC, Williams PS, Beckett R. Fractionating power in programmed field-flow fractionation: exponential sedimentation field decay. *Anal Chem.* 1987;59:28–37.
25. Brant J, Lecoanet H, Wiesner MR. Aggregation and deposition characteristics of fullerene nanoparticles in aqueous systems. *J Nanopart Res.* 2015;7:545–53.
26. Gigault J, Grassl B. Improving the understanding of fullerene (nC60) aggregate structures: fractal dimension characterization by static light scattering coupled to asymmetrical flow field flow fractionation. *J Colloid Interface Sci.* 2017;502:193–200.
27. Bendixen N, Losert S, Adlhart C, Lattuada M, Ulrich A. Membrane-particle interactions in an asymmetric flow field flow fractionation channel studied with titanium dioxide nanoparticles. *J Chromatogr A.* 2014;1334:92–100.
28. Du Q, Schimpf ME. Correction for particle-wall interactions in the separation of colloids by flow field-flow fractionation. *Anal Chem.* 2002;74:2478–85.
29. Baalousha M, Yang Y, Vance ME, Colman BP, McNeal S, Xu J, et al. Outdoor urban nanomaterials: the emergence of a new, integrated, and critical field of study. *Sci Total Environ.* 2016;557–558:740–53.
30. Andrady AL. Microplastics in the marine environment. *Mar Pollut Bull.* 2011;62:1596–605.
31. Eerkes-Medrano D, Thompson RC, Aldridge DC. Microplastics in freshwater systems: a review of the emerging threats, identification of knowledge gaps and prioritisation of research needs. *Water Res.* 2015;75:63–82.
32. Hidalgo-Ruz V, Gutow L, Thompson RC, Thiel M. Microplastics in the marine environment: a review of the methods used for identification and quantification. *Environ Sci Technol.* 2012;46:3060–75.
33. Gigault J, Pedrono B, Maxit B, Halle AT. Marine plastic litter: the unanalyzed nano-fraction. *Environ Sci Nano.* 2016;3:346–50.